

In-plane dielectric properties of epitaxial Ba_{0.7}Sr_{0.3}TiO₃ thin films grown on GaAs for tunable device application

Zhibin Yang and Jianhua Hao

Citation: *J. Appl. Phys.* **112**, 054110 (2012); doi: 10.1063/1.4749270

View online: <http://dx.doi.org/10.1063/1.4749270>

View Table of Contents: <http://jap.aip.org/resource/1/JAPIAU/v112/i5>

Published by the [American Institute of Physics](#).

Related Articles

Pyroelectric current measurements on PbZr_{0.2}Ti_{0.8}O₃ epitaxial layers
J. Appl. Phys. **112**, 104106 (2012)

Evolution of local work function in epitaxial VO₂ thin films spanning the metal-insulator transition
Appl. Phys. Lett. **101**, 191605 (2012)

Anisotropic electrical properties in bismuth layer structured dielectrics with natural super lattice structure
Appl. Phys. Lett. **101**, 012907 (2012)

Dielectric dynamics of epitaxial BiFeO₃ thin films
AIP Advances **2**, 022133 (2012)

Epitaxial growth of Pb(Zr_{0.53}Ti_{0.47})O₃ films on Pt coated magnetostrictive amorphous metallic substrates toward next generation multiferroic heterostructures
J. Appl. Phys. **111**, 064104 (2012)

Additional information on J. Appl. Phys.

Journal Homepage: <http://jap.aip.org/>

Journal Information: http://jap.aip.org/about/about_the_journal

Top downloads: http://jap.aip.org/features/most_downloaded

Information for Authors: <http://jap.aip.org/authors>

ADVERTISEMENT



AIP Advances

Special Topic Section:
PHYSICS OF CANCER

Why cancer? Why physics? [View Articles Now](#)

In-plane dielectric properties of epitaxial $\text{Ba}_{0.7}\text{Sr}_{0.3}\text{TiO}_3$ thin films grown on GaAs for tunable device application

Zhibin Yang and Jianhua Hao^{a)}

Department of Applied Physics and Materials Research Centre, The Hong Kong Polytechnic University, Hong Kong, People's Republic of China

(Received 15 May 2012; accepted 31 July 2012; published online 13 September 2012)

We have epitaxially deposited ferroelectric $\text{Ba}_{0.7}\text{Sr}_{0.3}\text{TiO}_3$ (BST) thin films grown on GaAs substrate via SrTiO_3 buffer layer by laser molecular beam epitaxy. Structural characteristics of the heterostructure were measured by various techniques. The in-plane dielectric properties of the heteroepitaxial structure under different applying frequency were investigated from -190 to 90°C , indicating Curie temperature of the BST film to be around 52°C . At room temperature, the dielectric constant of the heterostructure under moderate dc bias field can be tuned by more than 30% and K factor used for frequency agile materials is found to be close to 8. Our results offer the possibility to combine frequency agile electronics of ferroelectric titanate with the high-performance microwave capabilities of GaAs for room temperature tunable device application. © 2012 American Institute of Physics. [<http://dx.doi.org/10.1063/1.4749270>]

I. INTRODUCTION

Perovskite oxides are very attractive materials which can be used for a variety of devices.¹⁻³ Among these devices, frequency and phase agile microwave devices have widespread applications. For electric-field tuning, the ferroelectrics of choice are mostly $\text{Ba}_{1-x}\text{Sr}_x\text{TiO}_3$, where the Curie temperature depends on the Ba/Sr ratio, and can be adjusted from 40 K for SrTiO_3 (STO) to 398 K for pure BaTiO_3 .^{4,5} The high dielectric constant, low dielectric loss, and the dielectric nonlinearity are the materials parameters that enable such applications. To date, the fabrication of titanate-based tunable devices has been well done on single-crystal oxide substrates such as MgO and LaAlO_3 (LAO).⁶⁻⁸ However, the problems are the high cost of the substrates and the fact that oxide substrates of MgO and LAO are only available in small geometries, which are not suitable for mass production.⁹ Additionally, the use of oxide substrates requires mounting complicated hybrid microwave integrated circuits. Therefore, it is of great interest to combine the frequency agile electronics of ferroelectric titanates directly with the high-performance microwave capabilities of GaAs. This interest is also driven by the affordability and large-size availability of commercial GaAs wafers. Obviously, fabrication of high-quality heterostructures is the first step in the realization of new integrated devices. Unfortunately, the integration of perovskite titanates into the III-V's technology still represents a significant challenge. Compared to the growth of perovskite titanates on Si, there is limited work on the titanate/III-V's heteroepitaxial structures. Many properties and functionalities of the heterostructures are unknown. In our earlier work, epitaxial STO thin films were grown on GaAs substrates.¹⁰ It is known that STO with a cubic perovskite structure has a relatively large dielectric constant and a lattice parameter that is closely matched with a large number

of functional materials. Improved electrical properties of functional oxides grown on STO buffered GaAs are presented.^{11,12} Hence, it is of great interest to explore the heterostructure consisting of $\text{Ba}_{1-x}\text{Sr}_x\text{TiO}_3$ and GaAs, aiming at room temperature tunable device. In this work, we have successfully grown ferroelectric $\text{Ba}_{0.7}\text{Sr}_{0.3}\text{TiO}_3$ (BST) thin films on GaAs substrate via STO buffer layer by laser molecular beam epitaxy (MBE). Structural and dielectric nonlinearity of the heterostructure are presented.

II. EXPERIMENT

The BST thin films were deposited on STO buffered high resistivity GaAs (001) substrate ($\rho > 1 \times 10^6 \Omega \text{ m}$) by O_2 flowing pulsed laser MBE system with an operation wavelength of KrF ($\lambda = 248 \text{ nm}$). The distance between target and the substrate is 5 cm. The STO buffer layer was first deposited on GaAs substrate as described in our previous report.¹⁰ Briefly, the deposition temperature is set around 600°C for STO thin film grown on GaAs. To prevent the oxidation of GaAs occurring, the chamber was evacuated to a base pressure of $5 \times 10^{-5} \text{ Pa}$ during the STO thin-film deposition. The deposition time was 10 min when the laser repetition rate was kept at 1 Hz, resulting in an approximately 10 nm thick STO layer. After that, the STO/GaAs was heated up to 620°C and the oxygen partial pressure was fixed at 1 Pa for the subsequent BST deposition. A relatively small oxygen pressure used here is to avoid possible oxidation of GaAs, which could decrease the crystallinity of the heterostructure. The thickness of the BST thin film was around 300 nm. After deposition, the films were then *in situ* annealed in ambient of 200 Pa oxygen pressure for 1 h before being cooled down to room temperature in order to reduce the oxygen vacancies.

The crystallographic characterization was performed by a Rigaku SmartLab high resolution x-ray diffractometer (HRXRD). The surface morphology of the BST thin films was observed using an atomic force microscope (AFM)

^{a)}Author to whom correspondence should be addressed. Electronic mail: apjhao@inet.polyu.edu.hk.

(Digital Instrument Nanoscope IV) in tapping mode. Interdigital electrode (IDE) was used to test the in-plane dielectric properties of BST thin films. Standard photolithography was employed to make the IDE with 100-nm-thick Au top layer. The in-plane dielectric properties of BST thin film were measured using an HP 4294A impedance analyzer connected to an Oxford temperature controlled chamber (-190°C to 150°C). The dielectric constant can be obtained from the measured capacitances by using Gevorgian model.^{13,14}

III. RESULTS AND DISCUSSIONS

Figure 1(a) shows a typical θ - 2θ XRD scan of the thin films. As observed from the figure, only (00 l) peaks of the BST appear in the diffraction patterns besides the peaks from GaAs wafer. It suggests that the BST thin films have a single perovskite phase and are highly oriented along c -axis. Since the small thickness of STO layer, obvious peaks corresponding to STO can not be found in Figure 1. Rocking curve measurements indicate a full width at half maximum (FWHM) value of 1.1° in the inset of Fig. 1(a). This value is larger than that of the previously reported BST films on single-crystal substrates. For example, the FWHM values of BST thin films grown on MgO substrates and LAO substrates are around 0.54° and 0.15° , respectively.^{15,16} At room temperature, the lattice parameters for the bulk BST are $a = b = c = 3.965 \text{ \AA}$.⁶ Calculation based on Figure 1(a) results in c -axis lattice constants of 3.992 \AA and 5.653 \AA for BST thin film and GaAs substrate, respectively. It was observed that the lattice parameter of BST thin film is slightly larger than that of bulk BST, which suggests that the BST film suffered from a compressive strain caused by the lattice mismatch between BST and the underlying cubic STO buffer layer ($a = 3.903 \text{ \AA}$). In Figure 1(b), the off-axis Φ scans of the BST film and GaAs are presented, in which the (110) diffraction peak is used for the BST film. Only four peaks, 90° apart, are shown for the BST films, which are at the same angles with GaAs wafer. The measured results indicate the BST film is epitaxially grown on the (001) surface of STO and has an in-plane film-substrate orientation relationship of $[100]_{\text{BST}} \parallel [100]_{\text{STO}} \parallel [110]_{\text{GaAs}}$. Typical AFM images taken from the surface of the BST film in Figure 1(c) confirm the high quality structure of the BST films. The as-grown film has very smooth surface with a root-mean square roughness values of 1.60 nm from AFM measurement. Such good surface makes the thin films suitable for fabricating devices with in-plane electrodes. Investigation of the interfacial properties of BST/STO/GaAs is under way using transmission electron microscopy and x-ray photoelectron spectroscopy on our previously studied STO/Si.¹⁷ Preliminary results show that the interdiffusion may occur in the titanate/GaAs system.

In Figure 2, the dielectric constant and normalized dissipation factor of BST thin film deposited on STO/GaAs are plotted as a function of frequency at room temperature. The inset of Figure 2 shows the image of IDE configuration used for dielectric measurement. The pattern possesses a total of 21 fingers with figure length of $925 \mu\text{m}$, a finger width of

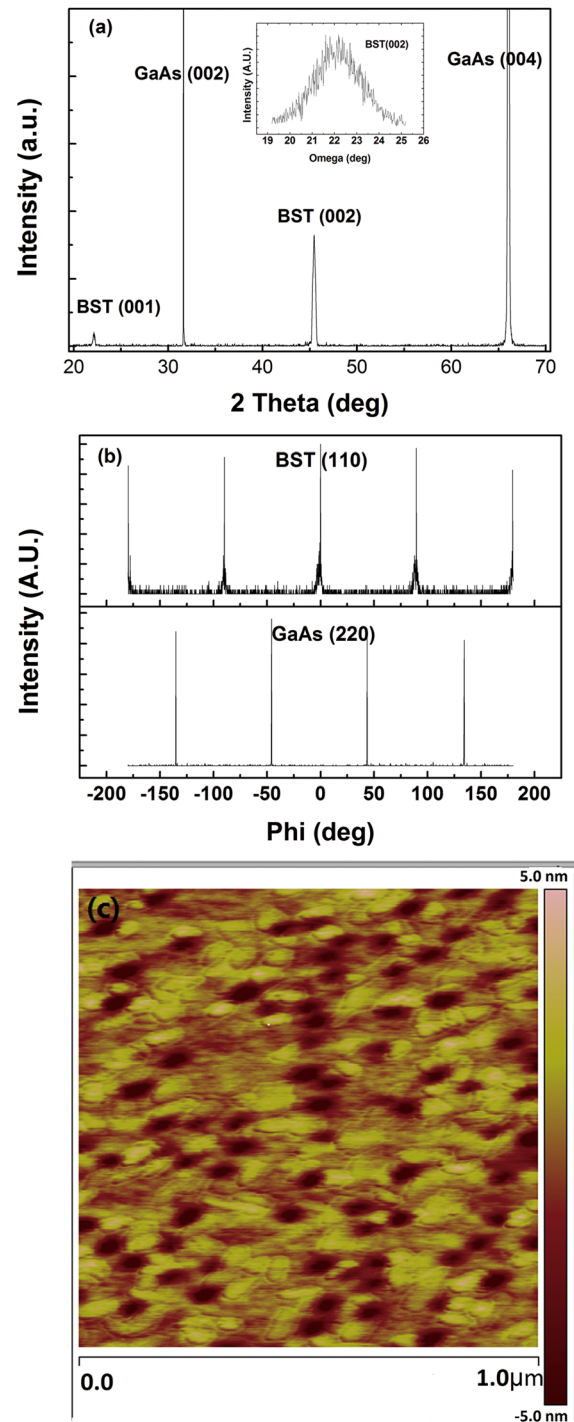


FIG. 1. (a) XRD pattern of BST/STO/GaAs (001) heterostructure. The inset shows the rocking curve of BST (002). (b) Phi scan of the (110) diffraction of the BST thin films on STO buffered GaAs substrate. (c) AFM image of the BST thin film on STO buffered GaAs.

$5 \mu\text{m}$, and a finger gap of $2 \mu\text{m}$. The relative permittivity of the films decreases with increased frequency. The dielectric loss of the film was found to be varied throughout the whole measured frequency. The loss tangent values are similar to those measured factor-frequency characteristics of BST thin film on bare high-resistivity silicon reported in the literature.¹⁸

Figure 3(a) shows the temperature-dependent in-plane dielectric constant ϵ of the BST thin film. The measurement

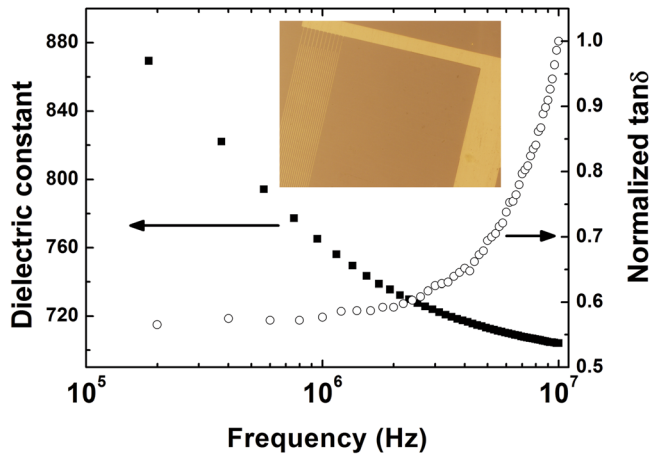


FIG. 2. Dielectric constant and normalized loss of 300 nm BST film as a function of frequency at room temperature. The inset is the image showing the IDEs used for dielectric measurement.

was conducted at four different frequencies as 1 kHz, 10 kHz, 100 kHz, and 1 MHz. The maximum dielectric constant at these four frequencies was found to be 1100, 980, 900, and 780, respectively. Almost same value of Curie temperature point is demonstrated for these four measuring frequencies, which exhibits from curves at $T_c \approx 52^\circ\text{C}$. The obtained value is about 19°C higher than that of the bulk BST material ($T_c = 33^\circ\text{C}$). The mechanism of shift in T_c of the BST thin film along the in-plane direction is attributed to the effect of in-plane tensile strain induced by the lattice misfit. The in-plane strain s of the BST thin film can be calculated by using an equation $s = (a_{\parallel} - a_0)/a_0$, where a_{\parallel} is the lattice parameter of the BST thin film and a_0 is the lattice parameter of bulk BST. Based on the lattice parameters, we

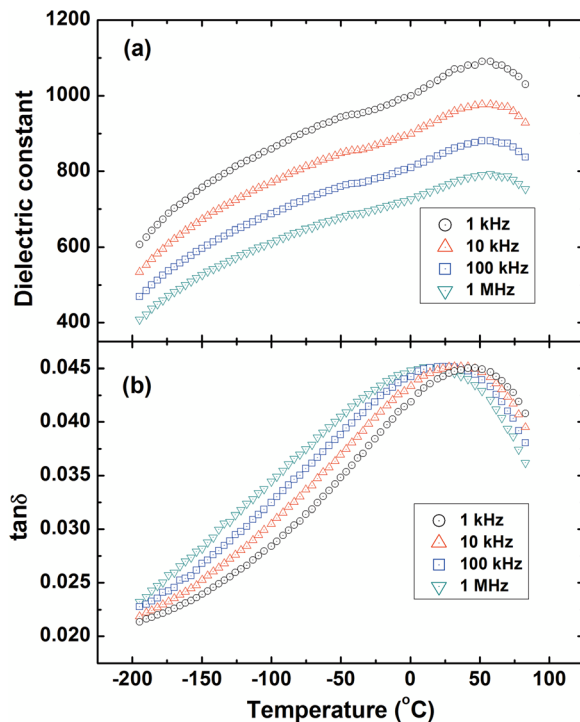


FIG. 3. (a) In-plane dielectric constant and (b) dielectric loss of BST thin film as a function of temperature.

calculated from XRD results and the value of s is found to be 0.68%. It should be noted that the shift in T_c of our BST/STO/GaAs heterostructure is not as significant as that observed in BST thin film grown on other substrates in the literature.⁶ Possible explanations for the difference could be (1) the compressive strain induced by the STO buffer layer is gradually relaxed as the film thickness increases, and (2) the oxygen deficiency in the heterostructure. Another possible cause for the shift of Curie temperature might be due to the deviated ratio of Ba/Sr. The corresponding loss tangent data are present in Figure 3(b). The value of $\tan\delta$ was found to be dependent on the temperature and frequency ranging from 0.021 to 0.045.

To examine the feasibility of making tunable devices by combining the frequency agile electronics of BST with the high-performance microwave capabilities of GaAs, we have measured the electric-field dependence of the dielectric constant and loss for the 300 nm BST film on STO/GaAs. As shown in Figure 4, the heterostructure exhibits a butterfly-shaped ϵ - E and $\tan\delta$ - E dependence at room temperature. The electric field E_m , at which ϵ is a maximum, is found to be $0.7\text{ V}/\mu\text{m}$. The maximum in-plane dielectric tunability is calculated to be 30% at 1 MHz under a moderate electric field of $10\text{ V}/\mu\text{m}$. The dielectric loss at zero field is relatively high, which may be explained by the ferroelectric phase induced by the strain.⁶ The commonly used figure of merit for the quality of frequency and phase agile materials is a simple approach for relating the tunability and dielectric loss in a tunable material, the so-called K factor defined as⁴

$$K = \frac{\epsilon(0) - \epsilon(E_{\text{max}})}{\epsilon(0)} \frac{1}{(\tan\delta)_{\text{max}}}, \quad (1)$$

where $(\tan\delta)_{\text{msx}}$ is the maximum loss under all the applied fields. The K factor at room temperature was obtained to be ~ 8 based on the result in Figure 4. The obtained tunability and K factor of our BST films grown on GaAs are lower compared to the reported BST film grown on MgO.⁶ However, our results are superior than the performance measured from BST film grown on high resistivity Si substrate.¹⁸

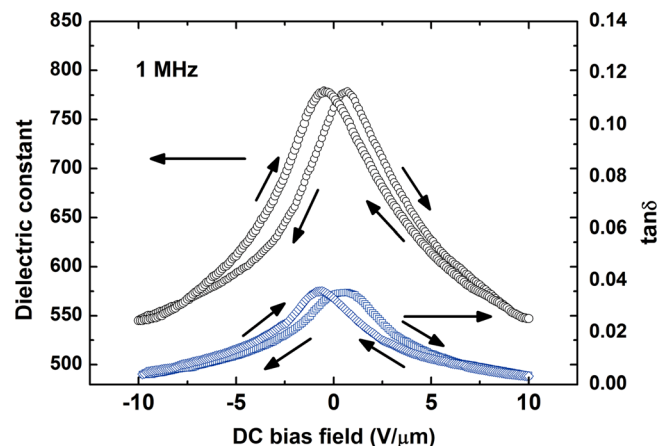


FIG. 4. In-plane room-temperature dielectric constant and loss of BST thin film as a function of electric field at 1 MHz.

IV. CONCLUSIONS

In conclusion, heterostructure of BST/STO/GaAs were fabricated by using O₂ flowing laser molecular beam epitaxy technique. The lattice orientation and surface structure have been confirmed by x-ray diffraction and AFM. The dielectric properties were also studied. Curie temperature point of BST thin film shifts to around 19 °C higher than that of BST bulk material. Butterfly-shaped C-V characteristic curves were observed. A relatively large dielectric tunability of 30% was found at 1 MHz. By considering the high-performance microwave capabilities and large-size availability of commercial GaAs, this work exhibits that the BST/STO/GaAs heterostructure can be processed to be a new system for tunable microwave applications.

ACKNOWLEDGMENTS

This research was supported by the grants from the Research Grants Council of Hong Kong (GRF Project No. PolyU500910) and ITS 029/11.

¹I. Vrejoiu, M. Alexe, D. Hesse, and U. Gösele, *Adv. Funct. Mater.* **18**, 3892 (2008).

²T. Yajima, Y. Hikita, and H. Y. Hwang, *Nature Mater.* **10**, 198 (2011).

- ³J. H. Hao, X. T. Zeng, and H. K. Wong, *J. Appl. Phys.* **79**, 1810 (1996).
- ⁴X. X. Xi, H. C. Li, W. Si, A. A. Sirenko, I. A. Akimov, J. R. Fox, A. M. Clark, and J. Hao, *J. Electroceram.* **4**, 393 (2000).
- ⁵C. L. Chen, J. Shen, S. Y. Chen, G. P. Luo, C. W. Chu, F. A. Miranda, F. W. Van Keuls, J. C. Jiang, E. I. Meletis, and H. Chang, *Appl. Phys. Lett.* **78**, 652 (2001).
- ⁶D. Y. Wang, Y. Wang, X. Y. Zhou, H. L. W. Chan, and C. L. Choy, *Appl. Phys. Lett.* **86**, 212904 (2005).
- ⁷J. S. Wu, C. L. Jia, K. Urban, J. H. Hao, and X. X. Xi, *J. Mater. Res.* **16**, 3443 (2001).
- ⁸Q. X. Jia, B. H. Park, B. J. Gibbons, J. Y. Huang, and P. Lu, *Appl. Phys. Lett.* **81**, 114 (2002).
- ⁹M. W. Cole, P. C. Joshi, M. Wood, and R. L. Pfeffer, *J. Appl. Phys.* **92**, 3967 (2002).
- ¹⁰Z. P. Wu, W. Huang, K. H. Wong, and J. H. Hao, *J. Appl. Phys.* **104**, 054103 (2008).
- ¹¹W. Huang, Z. P. Wu, and J. H. Hao, *Appl. Phys. Lett.* **94**, 032905 (2009).
- ¹²W. Huang, J. Y. Dai, and J. H. Hao, *Appl. Phys. Lett.* **97**, 162905 (2010).
- ¹³Y. Wang, Y. L. Cheng, K. C. Cheng, H. L. W. Chan, and C. L. Choy, *Appl. Phys. Lett.* **85**, 1580 (2004).
- ¹⁴S. S. Gevorgian, T. Matinsson, P. L. J. Linner, and E. L. Kollberg, *IEEE Trans. Microwave Theory Tech.* **44**, 896 (1996).
- ¹⁵S. E. Moon, E.-K. Kim, M.-H. Kwak, H.-C. Ryu, and Y.-T. Kim, *Appl. Phys. Lett.* **83**, 2166 (2003).
- ¹⁶H.-J. Gao, C. L. Chen, B. Rafferty, S. J. Pennycook, G. P. Luo, and C. W. Chu, *Appl. Phys. Lett.* **75**, 2542 (1999).
- ¹⁷J. H. Hao, J. Gao, Z. Wang, and D. P. Yu, *Appl. Phys. Lett.* **87**, 131908 (2005).
- ¹⁸H.-S. Kim, H.-G. Kim, I.-D. Kim, K.-B. Kim, and J.-C. Lee, *Appl. Phys. Lett.* **87**, 212903 (2005).